



Published in final edited form as:

Science. 2012 May 4; 336(6081): 604–608. doi:10.1126/science.1216753.

Radio-Wave Heating of Iron Oxide Nanoparticles Can Regulate Plasma Glucose in Mice

Sarah A. Stanley¹, Jennifer E. Gagner², Shadi Damanpour¹, Mitsukuni Yoshida³, Jonathan S. Dordick⁴, and Jeffrey M. Friedman^{1,5,*}

¹Laboratory of Molecular Genetics, Rockefeller University, New York, NY 10065, USA

²Department of Materials Science and Engineering, Rensselaer Nanotechnology Center, Rensselaer Polytechnic Institute, Troy, NY 12180, USA

³Elizabeth and Vincent Meyer Laboratory of Systems Cancer Biology, Rockefeller University, New York, NY 10065, USA

⁴Department of Chemical and Biological Engineering, Department of Biology, Center for Biotechnology and Interdisciplinary Studies, Rensselaer Polytechnic Institute, Troy, NY 12180, USA

⁵Howard Hughes Medical Institute, New York, NY 10065, USA

Abstract

Medical applications of nanotechnology typically focus on drug delivery and biosensors. Here, we combine nanotechnology and bioengineering to demonstrate that nanoparticles can be used to remotely regulate protein production in vivo. We decorated a modified temperature-sensitive channel, TRPV1, with antibody-coated iron oxide nanoparticles that are heated in a low-frequency magnetic field. When local temperature rises, TRPV1 gates calcium to stimulate synthesis and release of bioengineered insulin driven by a Ca²⁺-sensitive promoter. Studying tumor xenografts expressing the bioengineered insulin gene, we show that exposure to radio waves stimulates insulin release from the tumors and lowers blood glucose in mice. We further show that cells can be engineered to synthesize genetically encoded ferritin nanoparticles and inducibly release insulin. These approaches provide a platform for using nanotechnology to activate cells.

Remote activation of specific cells to trigger gene expression and peptide release in vivo could provide a useful research tool and, in time, potentially provide a means for regulated expression of proteins in clinical settings. Cell activation by direct stimulation with electrodes (1) is limited by nonspecific and variable activation, the need for permanent implants, and potential tissue damage (2, 3). Ion channels, such as channelrhodopsin, regulate intracellular ions and cell activity (4) with anatomical specificity and temporal control, but, because light waves do not penetrate tissue, implanted devices are required. In contrast, low and medium radio frequencies (RFs) can penetrate deep tissues with minimal energy absorption (5, 6). Unlike tissue, metal nanoparticles absorb energy and heat in response to RF (7, 8). This heating, which depends on particle composition and size and RF field strength, (9) can be converted into a cellular signal by using a temperature-sensitive

*To whom correspondence should be addressed. friedj@mail.rockefeller.edu.

www.sciencemag.org/cgi/content/full/336/6081/604/DC1

Materials and Methods

Supplementary Text

Figs. S1 to 10

References (28–35)

channel to allow ion entry. Targeting of nanoparticles can be achieved by coating with specific antibodies (10, 11) to induce cell-specific, cell membrane temperature changes that are then transduced by a temperature sensitive channel into cellular responses.

We have applied these principles to develop a system that allows remote activation of protein production by engineered cells in vitro and in vivo. The method (Fig. 1A) uses iron oxide nanoparticles (FeNPs) that are coated with antibodies against His (anti-His) and that bind a modified TRPV1 channel with an extracellular His \times 6 epitope tag (TRPV1^{His}). We reasoned that, with RF treatment, local heating of bound anti-His FeNPs would activate the temperature-sensitive TRPV1, resulting in a calcium current to activate a Ca²⁺-sensitive promoter placed upstream of a modified human insulin reporter gene.

We used FeNPs for the following reasons: They heat at 465 kHz, a relatively low frequency that minimizes tissue heating; particles of 20 nm or less diffuse in the extracellular space (11–13); and these particles can be derivatized with antibodies. At 465 kHz (5 mT), substantial heating was observed for 20- and 25-nm FeNP suspensions (Fig. S1). A 20-nm FeNP suspension had an initial heating rate of 0.15°C/s and a specific absorption rate (SAR) of 0.63 W/g, whereas the SAR of water at this field frequency and strength was less than 0.004 W/g. As shown by electron microscopy, a His-tag insertion into the first extracellular loop of TRPV1 provided a site for significant and specific FeNP binding (Fig. S2) with direct heat transfer to the adjacent channel (Fig. S3). Human embryonic kidney (HEK) 293T cells expressing TRPV1^{His} and decorated with 20 nM FeNPs conjugated to anti-His showed a significant increase in intracellular Ca²⁺ after 10s of RF exposure (Fig. S2D).

Calcium entry was next used to induce gene expression via a novel synthetic 5' regulatory region composed of three Ca²⁺ response elements in cis: serum response element (SRE), cyclic adenosine monophosphate response element (CRE), and nuclear factor of activated T cell response element (NFAT RE) (14, 15) with a minimal promoter. This was placed upstream of a modified human proinsulin gene with furin cleavage sites replacing beta-cell-specific convertase cleavage sites to allow insulin processing in non-beta cells (16) (Fig. S4A).

HEK 293T cells expressing the Ca²⁺-dependent human insulin construct and TRPV1^{His} were incubated with functionalized FeNPs. RF treatment of the FeNP-decorated cells resulted in a significant increase in proinsulin release (RF-treated 671 \pm 235% (SEM) basal versus 100 \pm 13.9% for controls, $P < 0.02$) and insulin gene expression (RF-treated 2.20 \pm 0.53 insulin gene expression relative to basal versus 1.0 \pm 0.18 for controls, $P < 0.05$). These were blocked by the TRP channel inhibitor, ruthenium red (Fig. 1B). There was a trend toward an increase in proinsulin release after 15 min of RF treatment (likely through release of a small pool of preformed insulin-containing vesicles), with significant proinsulin release at 1 hour when insulin gene expression had also significantly increased (Fig. 1C). Control studies confirmed that proinsulin release required all system components (i.e., TRPV1, nanoparticles, and RF magnetic field) and that RF-dependent insulin secretion was confined to FeNP-decorated cells (Fig. S4, B and C). RF treatment induced NFAT translocation into the nucleus, and RF-dependent proinsulin release was blocked by a calcineurin inhibitor, tacrolimus (Fig. S4, D and E). RF treatment of cells incubated with FeNPs (1 to 8 mg/ml) did not induce apoptosis as assessed by immunohistochemistry for active caspase 3 (17) and terminal deoxynucleotidyl transferase-mediated deoxyuridine triphosphate nick end labeling (TUNEL) (18) (Fig. S4, F and G). We also showed that RF could stimulate proinsulin release from mouse embryonic stem cells expressing TRPV1^{His} and the Ca²⁺-dependent human insulin construct (Fig. S5).

Next, we compared our single-component system to a multicomponent system previously reported (19) and composed of (i) a membrane-tethered biotin acceptor protein, (ii) a bacterial biotin ligase to biotinylate this protein to enable binding of (iii) streptavidin-coated nanoparticles, and (iv) a wild-type TRPV1 as the effector. Although this system induced Ca^{2+} entry in vitro and activated endogenous temperature sensing of *Caenorhabditis elegans* neurons, the complete system was not tested in vivo because the exogenous TRPV1 channel was not used in this prior study. We found that our single-component system had denser nanoparticle binding, faster calcium entry, and a trend toward more robust pro-insulin release (Fig. S6, A and G). These attributes led us to test the single-component TRPV1^{His} system in vivo in mice by using xenografts of engineered neuroendocrine PC12 cells, which robustly secrete peptides via the regulated pathway for protein secretion.

Exposure of a PC-12 cell line stably expressing TRPV1^{His} and the calcium-dependent human insulin construct (PC12-TRPV1^{His}-Ins) to RF after FeNP application significantly increased proinsulin release and insulin gene expression in vitro (Fig. S7, A to D). The PC12-TRPV1^{His}-Ins cells were injected subcutaneously into the flank of nude mice to form tumors (Fig. S7F). There was no change in plasma glucose with tumor growth (Fig. S7E). Phosphate-buffered saline (PBS) or FeNP (50- μl total volume, nanoparticle concentration of 8 mg/ml) were injected into the tumors of fasted mice, and blood glucose and plasma insulin were measured before, during, and after RF application (see Fig. S8A for protocol). RF treatment resulted in a significant decrease in blood glucose in nanoparticle-treated PC12-TRPV1^{His}-Ins tumor mice (Fig. 2A) (The change in blood glucose at 30 min for FeNP-treated was -53.6 ± 8.90 mg/dl, versus PBS-treated, -11.0 ± 9.72 mg/dl; $P < 0.005$. At 45 min, the change in blood glucose for FeNP-treated mice was -60.9 ± 11.6 mg/dl versus PBS-treated -9.74 ± 8.52 mg/dl; $P < 0.005$. At 60 min, the change in blood glucose for FeNP-treated mice was -55.1 ± 13.2 mg/dl versus PBS-treated, -6.24 ± 15.3 mg/dl; $P < 0.0001$). There was also a highly significant difference in the cumulative change in blood glucose (area under the curve, AUC) between PBS-treated and FeNP-treated PC12-TRPV1^{His}-Ins tumor mice over the course of the study (Fig. 2B) [AUC (0 to 120 min) for PBS-treated was 272 ± 692 mg/dl min versus FeNP-treated, -2695 ± 858.3 mg/dl min; $P < 0.002$]. Plasma insulin was significantly increased after RF treatment in FeNP-treated but not PBS-injected mice (Fig. 2C) [plasma insulin for FeNP-treated (-30 min) was 2.26 ± 0.76 $\mu\text{I-U/ml}$ (where 1 $\mu\text{I-U/ml}$ = 0.006 pmol/l) versus FeNP-treated (30 min), 3.25 ± 0.64 $\mu\text{I-U/ml}$; $P < 0.05$. PBS-treated (-30 min) was 1.83 ± 0.38 $\mu\text{I-U/ml}$ versus PBS-treated (30 min), 1.75 ± 0.36 $\mu\text{I-U/ml}$]. Lastly, insulin gene expression was significantly increased in RF-treated, FeNP-injected tumors (Fig. 2D) (relative insulin gene expression in FeNP-treated, no RF samples was 1.0 ± 0.2 versus FeNP-treated with RF, 2.0 ± 0.3 , $P < 0.05$) without increasing c-fos expression (fig. S8B). Core temperature did not change significantly with RF exposure, and the intratumoral temperatures (23° to 31°C) remained well below the 42°C threshold of TRPV1, suggesting that cell activation is due to localized, cell surface-specific gating of TRPV1. There was no difference in apoptosis between FeNP-injected tumors in the presence or absence of the RF magnetic field (fig. S8, C and D). A significant decrease in blood glucose was also seen with serial FeNP injection and RF treatment (fig. S8, E and F). To confirm that the effects on blood glucose were not due to nonspecific insulin release via thermal effects of nanoparticles on the tumor, we repeated the in vivo study, first in mice injected with PC12 cells expressing the Ca^{2+} -dependent human insulin construct but not TRPV1^{His} and then in mice with tumors expressing TRPV1^{His} and insulin but injected with nanoparticles without anti-His conjugation. There was no significant effect on blood glucose in either study after PBS or FeNP injection and RF treatment despite similar intra-tumoral temperatures (fig. S9, A to D).

The above approach requires direct application of nanoparticles to TRPV1 expressing cells by incubation (in vitro) or injection (in vivo). An alternative is to engineer cells to

synthesize nanoparticles intracellularly. For this purpose, we chose the iron storage protein ferritin, which forms a naturally occurring paramagnetic iron nanoparticle (20, 21) (Fig. 3A and fig. S10). Ferritin has been stably overexpressed in mice for over 2 years without evident pathology (22). A fusion peptide of ferritin light chain, flexible linker region, and ferritin heavy chain fixes the ratio of light to heavy chains and increases iron binding (23). Transfecting cells with ferritin fusion protein resulted in 12.6 ± 2.86 ferritin particles per $0.2 \mu\text{m}^2$ with an average distance to the cell membrane of 60.3 ± 2.85 nm (fig. S10B). RF treatment of cells expressing the ferritin fusion protein, TRPV1, and Ca^{2+} -dependent human insulin significantly increased proinsulin release (RF treated, $457 \pm 103\%$ basal versus control, $100 \pm 14.9\%$ basal; $P < 0.005$) and insulin gene expression (relative insulin gene expression for RF treated, 1.58 ± 0.19 versus control, 1.0 ± 0.17 ; $P < 0.05$) (Fig. 3B). Intracellularly generated FeNPs were roughly two-thirds as effective in stimulating proinsulin release as exogenous FeNP. In the absence of TRPV1, insulin secretion and gene expression were unchanged in ferritin-expressing cells. Thus, ferritin expression may provide a genetically encoded source of nanoparticles for RF-mediated cell activation.

We have shown that both externally applied and endogenously synthesized nanoparticles can be heated by radio waves to remotely activate insulin gene expression and secretion. RF-mediated cell activation does not require a permanent implant, and the cells to be activated can in principle be localized (when using exogenous nanoparticles) or dispersed (by using genetically encoded nanoparticles). Genetically encoded ferritin nanoparticles may also provide a continuous source of nanoparticles for cell activation.

The use of an epitope-tagged TRPV1 with antibody-coated nanoparticles resulted in high nanoparticle density in proximity to the channel and could gate calcium in response to power levels of a 465-kHz RF field that are within Food and Drug Administration guidelines (24, 25). The use of a single construct for particle binding and calcium entry also simplifies DNA delivery using viral vectors or other approaches (26). Lastly, an epitope-tagged channel offers the possibility of activating distinct cell populations in the same animal with different RFs to selectively and independently heat nanoparticles bound to cell specific tags. For endogenous particles, mutations of ferritin that alter the metal it encapsulates could potentially enable combinatorial cell activation (27).

In summary, we have developed a noninvasive, nonpharmacological means for cell stimulation and validated it in vitro and in vivo. This system provides a useful tool for basic research and represents an initial step toward noninvasive regulation of protein production for possible therapeutic purposes. If a practical means for delivery of the nanoparticles can be established, this approach could theoretically be used to treat protein deficiencies by providing regulated expression of proteins that are difficult to synthesize or to deliver [such as central nervous system (CNS) replacement of hexosaminidase A for Tay-Sachs] or to allow CNS delivery of recombinant antibodies to treat brain metastases. This approach could also potentially enable the activation of other Ca^{2+} -dependent processes, such as muscle contraction or firing of action potentials.

Supplementary Material

Refer to Web version on PubMed Central for supplementary material.

Acknowledgments

We thank Friedman laboratory members for helpful discussions, S. Korres for assistance with manuscript preparation, S. Tavazoie for helpful discussions, R. Toledo-Crow and S. Abeytunge for assistance with RF technology, and the staff of the Rockefeller University Electron Microscopy Resource center for their technical

support in imaging. This project was supported by funding from the JPB Foundation and grant no. R01 GM095654 from the NIH. The authors have filed a patent related to this work.

References and Notes

1. Gellhorn E, Cortell R, Feldman J. *Science*. 1940; 92:288. [PubMed: 17802522]
2. Stock G, Sturm V, Schmitt HP, Schlör KH. *Acta Neurochir (Wien)*. 1979; 47:123. [PubMed: 112839]
3. McIntyre CC, Grill WM. *J Neurophysiol*. 2002; 88:1592. [PubMed: 12364490]
4. Boyden ES, Zhang F, Bamberg E, Nagel G, Deisseroth K. *Nat Neurosci*. 2005; 8:1263. [PubMed: 16116447]
5. Young JH, Wang MT, Brezovich I. *Electron Lett*. 1980; 16:358.
6. Strauffer PR, Cetas TC, Jones RC. *IEEE Trans Biomed Eng*. 1984; 31:235. [PubMed: 6706353]
7. Richardson HH, et al. *Nano Lett*. 2006; 6:783. [PubMed: 16608284]
8. Hamad-Schifferli K, Schwartz JJ, Santos AT, Zhang S, Jacobson JM. *Nature*. 2002; 415:152. [PubMed: 11805829]
9. Fortin JP, et al. *J Am Chem Soc*. 2007; 129:2628. [PubMed: 17266310]
10. Samanta B, et al. *J Mater Chem*. 2008; 18:1204. [PubMed: 19122852]
11. Wang AZ, et al. *Expert Opin Biol Ther*. 2008; 8:1063. [PubMed: 18613759]
12. DeFalco J, et al. *Science*. 2001; 291:2608. [PubMed: 11283374]
13. Thorne RG, Nicholson C. *Proc Natl Acad Sci USA*. 2006; 103:5567. [PubMed: 16567637]
14. Hardingham GE, Bading H. *Microsc Res Tech*. 1999; 46:348. [PubMed: 10504212]
15. Rao A. *Nat Immunol*. 2009; 10:3. [PubMed: 19088731]
16. Shifrin AL, Auricchio A, Yu QC, Wilson J, Raper SE. *Gene Ther*. 2001; 8:1480. [PubMed: 11593361]
17. Tewari M, et al. *Cell*. 1995; 81:801. [PubMed: 7774019]
18. Gavrieli Y, Sherman Y, Ben-Sasson SA. *J Cell Biol*. 1992; 119:493. [PubMed: 1400587]
19. Huang H, Delikanli S, Zeng H, Ferkey DM, Pralle A. *Nat Nanotechnol*. 2010; 5:602. [PubMed: 20581833]
20. Farrant JL. *Biochim Biophys Acta*. 1954; 13:569. [PubMed: 13159997]
21. Sana B, Johnson E, Sheah K, Poh CL, Lim S. *Biointerphases*. 2010; 5:FA48. [PubMed: 21171713]
22. Ziv K, et al. *NMR Biomed*. 2010; 23:523. [PubMed: 20175142]
23. Iordanova B, Robison CS, Ahrens ET. *J Biol Inorg Chem*. 2010; 15:957. [PubMed: 20401622]
24. Halperin, D., et al. *Proceedings of the 2008 IEEE Symposium on Security and Privacy*; Oakland, CA. 18 to 21 May 2008; p. 129-142.
25. Hanna, SA. paper presented at the Third International Symposium on Medical Information and Communication Technology; Montreal, Canada. 24 to 27 February 2009;
26. Nathwani AC, et al. *N Engl J Med*. 2011; 365:2357. [PubMed: 22149959]
27. Butts CA, et al. *Biochemistry*. 2008; 47:12729. [PubMed: 18991401]

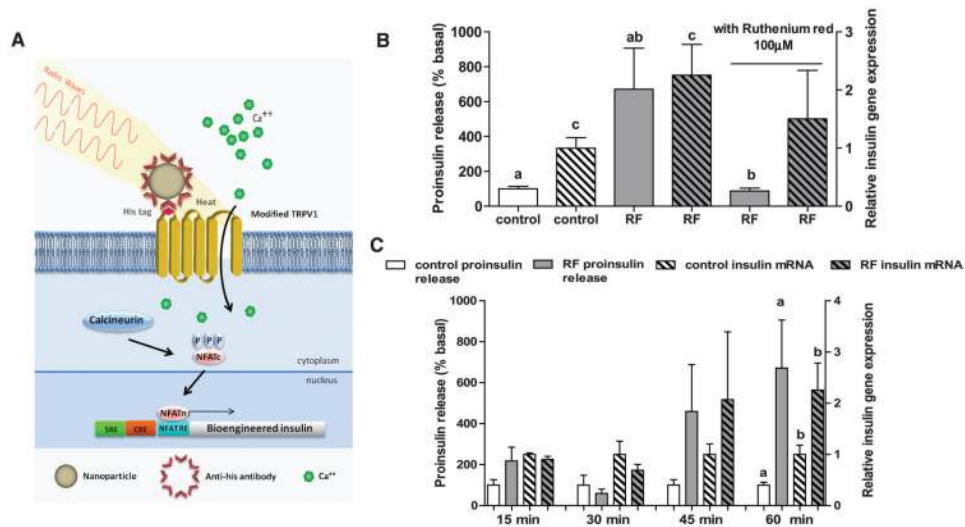


Fig. 1. Nanoparticles induced cell excitation to increase insulin expression and release in vitro. **(A)** Schema of nanoparticle-induced cell activation and gene expression. Antibody-coated ferrous oxide nanoparticles bind to a unique epitope, His \times 6, in the first extracellular loop of the temperature-sensitive TRPV1 channel. Exposure to a RF field induces local nanoparticle heating, which opens temperature-sensitive TRPV1 channels. Calcium entry triggers downstream pathways, such as activation of calcineurin, leading to dephosphorylation of NFAT and translocation to the nucleus. Here, NFAT binds to upstream response elements to initiate gene expression of a bioengineered human insulin gene. Additional calcium-dependent signal transduction pathways also stimulate gene expression via binding to SRE and CRE. P indicates a phosphate group. **(B)** RF treatment increases proinsulin release and insulin gene expression in vitro. Nanoparticle-decorated HEK293T cells transfected with TRPV1^{His} and calcium-dependent insulin show a significant increase in proinsulin release and insulin gene expression with RF treatment that is blocked by the TRP antagonist ruthenium red. (Columns marked with the same letter indicate significance, $P < 0.05$. Error bars indicate SEM) **(C)** Time courses of proinsulin release and insulin gene expression from nanoparticle-decorated HEK293T cells transfected with TRPV1^{His} and calcium-dependent insulin with RF treatment.

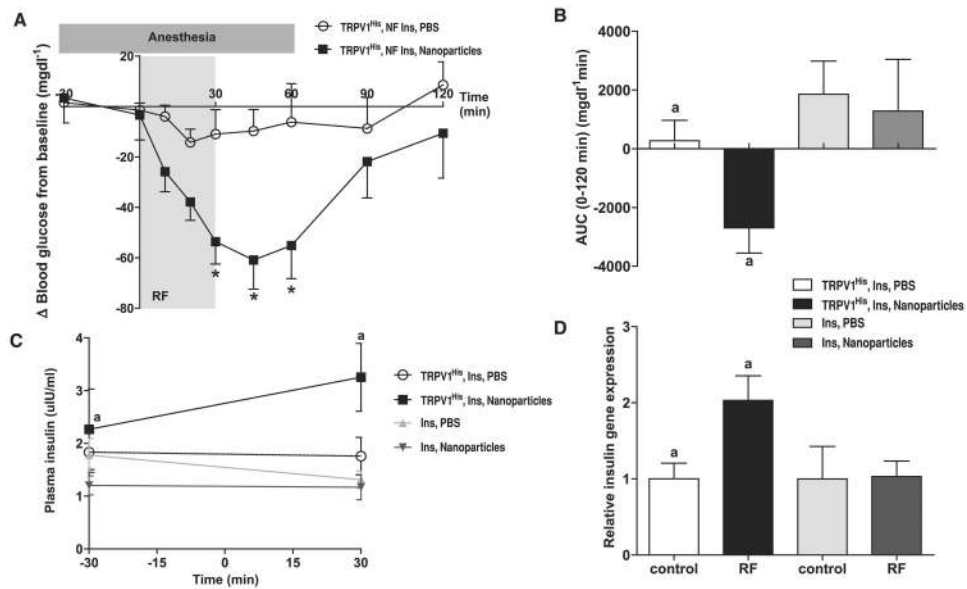


Fig. 2. Nanoparticle regulation of blood glucose in vivo. **(A)** Effects of RF treatment on blood glucose in PBS and nanoparticle-treated mice with tumors expressing TRPV1^{His} and calcium-dependent human insulin. RF treatment significantly reduces blood glucose in nanoparticle-treated mice compared with that of PBS-treated mice. (Asterisks indicate $P < 0.05$. Error bars indicate SEM.) **(B)** RF treatment of mice with tumors expressing TRPV1^{His} and calcium-dependent human insulin injected with nanoparticles significantly reduces blood glucose over the course of the study as assessed by the area under the curve. There is no effect in mice with tumors expressing calcium-dependent insulin alone without TRPV1^{His}. (Same letter indicates $P < 0.05$.) **(C)** Plasma insulin is significantly increased by RF treatment in nanoparticle-treated but not PBS-treated mice with tumors expressing TRPV1^{His} and calcium-dependent human insulin. There is no effect in mice with tumors expressing calcium-dependent insulin alone without TRPV1^{His}. (Same letter indicates $P < 0.05$.) **(D)** Insulin gene expression is significantly increased in the tumors expressing TRPV1^{His} and calcium-dependent human insulin treated with nanoparticles and RF magnetic field but not in tumors expressing calcium-dependent human insulin alone without TRPV1^{His}.

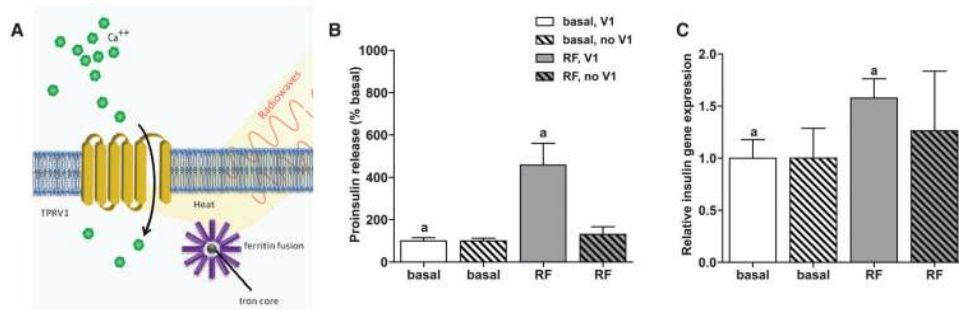


Fig. 3. Intracellular nanoparticle synthesis and cell activation. (A) Schema of intracellular nanoparticle synthesis and cell activation. A ferritin fusion protein is composed of a ferritin light chain fused to ferritin heavy chain with a flexible linker region. Heating of the iron core by a RF magnetic field opens the TRPV1 channel to trigger calcium entry, as previously described. (B) RF treatment increases proinsulin release in vitro. HEK293T cells transiently transfected with TRPV1, ferritin, and calcium-dependent human insulin show a significant increase in proinsulin release in response to RF treatment. (Same letter indicates significance, $P < 0.05$.) RF treatment does not increase proinsulin release from cells expressing ferritin in the absence of TRPV1. (C) RF treatment increases insulin gene expression in vitro. Insulin gene expression is significantly increased by RF treatment in cells transfected with TRPV1, ferritin, and calcium-dependent human insulin. (Same letter indicates significance, $P < 0.05$.) RF treatment does not increase insulin gene expression in cells expressing ferritin in the absence of TRPV1.